

Planetary waves in a stratified ocean of variable depth. Part 2. Continuously stratified ocean

By A. V. BOBROVICH AND G. M. REZNIK

P. P. Shirshov Institute of Oceanology, Russian Academy of Sciences, Krasikova,
23, 117218 Moscow, Russia

(Received 22 July 1996 and in revised form 15 December 1998)

Linear Rossby waves in a continuously stratified ocean over a corrugated rough-bottomed topography are investigated by asymptotic methods. The main results are obtained for the case of constant buoyancy frequency. In this case there exist three types of modes: a topographic mode, a barotropic mode, and a countable set of baroclinic modes. The properties of these modes depend on the type of mode, the relative height δ of the bottom bumps, the wave scale L , the topography scale L_b and the Rossby scale L_i . For small δ the barotropic and baroclinic modes are transformed into the ‘usual’ Rossby modes in an ocean of constant depth and the topographic mode degenerates. With increasing δ the frequencies of the barotropic and topographic modes increase monotonically and these modes become close to a purely topographic mode for sufficiently large δ . As for the baroclinic modes, their frequencies do not exceed $O(\beta L)$ for any δ . For large δ the so-called ‘displacement’ effect occurs when the mode velocity becomes small in a near-bottom layer and the baroclinic mode does not ‘feel’ the actual rough bottom relief. At the same time, for some special values of the parameters a sort of resonance arises under which the large- and small-scale components of the baroclinic mode intensify strongly near the bottom.

As in the two-layer model, a so-called ‘screening’ effect takes place here. It implies that for $L_b \ll L_i$ the small-scale component of the mode is confined to a near-bottom boundary layer $(L_b/L_i)H$ thick, whereas in the region above the layer the scale L of motion is always larger than or of the order of L_i .

1. Introduction

Density stratification and bottom relief produce a strong effect on the dynamics of low-frequency planetary waves in the ocean. The stratification is responsible for the existence of a countable number of vertical wave modes, whereas the topography modifies the dispersion relation and gives rise to topographic waves. Investigation of the topography effects is a complicated problem, and significant progress in its consideration has been made only for the case of a one-dimensional relief when the isobaths are parallel straight lines. The initial work was done by Rhines & Bretherton (1973), who examined the propagation of barotropic quasi-geostrophic oscillations of scale L over a sinusoidal bottom relief with horizontal scale L_b . The most important result of their work is that the rough corrugated relief supports propagating waves with $L > L_b$ even in the absence of the β -effect. Volosov (1976*a, b*) generalized these results to the nonlinear case. The stratified case was considered by Suarez (1971), McWilliams (1974), Volosov & Zhdanov (1980*a, b*, 1982, 1983), and Zhdanov (1987). The case of a random corrugated relief in a barotropic ocean was analysed numerically

by Sengupta, Piterbarg & Reznik (1992). All these works (except the last one) use the following constraints on the wave parameters:

$$\frac{\beta L}{f_0} \lesssim \frac{\sigma}{f_0} \sim \frac{\Delta h}{H} \sim \frac{L_b}{L} \ll 1, \quad (1.1)$$

where σ is the wavefrequency, f_0 is the local Coriolis parameter, $\beta = df/dy$, Δh is a typical height of the relief irregularities, and H is the mean ocean depth.

Reznik (1986), Samelson (1992), and Reznik & Tsybaneva (1999, referred to hereafter as Part 1) carried out a detailed investigation of waves in a two-layer ocean and found some new effects. They showed that in a two-layer ocean besides waves with frequencies satisfying (1.1) there always exists a wave with frequency

$$\frac{\sigma}{f_0} = O\left(\frac{\beta L}{f_0}\right) \quad (1.2)$$

even in the case of a high relief inhomogeneity where

$$\frac{\sigma}{f_0} \sim \frac{\beta L}{f_0} \ll \frac{\Delta h}{H}. \quad (1.3)$$

This wave exists due to the stratification, and therefore it is called the baroclinic mode. For small Δh when $\Delta h/H \ll \beta L/f_0$ this mode is transformed into the ‘usual’ baroclinic Rossby mode in a two-layer ocean of constant depth. But if $\Delta h/H$ is sufficiently large so that (1.3) holds, then the baroclinic wave is confined mainly to the upper layer as if this wave does not ‘feel’ the actual bottom and ‘interprets’ the interface between the layers as a bottom. In this case the motion in the lower layer is very weak, although it is necessarily present. This is the so-called ‘displacement’ effect, which is of great interest because the concentration of mesoscale motion in an upper layer over strong relief inhomogeneities has been observed many times in the real ocean (Wunsch 1981, 1983; Dickson 1983).

Another important effect (the so-called ‘screening’ effect) is that for $L_b < L_i$ (the internal Rossby scale) the wave component generated by the topography is confined to the lower layer, whereas in the upper layer the scale of motion L is always greater than or of the order of L_i (also see McWilliams 1974; Zhdanov 1987).

The present paper generalizes some results of the works by Reznik and Tsybaneva to the case of a continuously stratified ocean. For simplicity, the buoyancy frequency is assumed to be constant. In §2 the model under consideration is described. After that an asymptotic theory of Rossby waves over a rough bottom topography is developed (§§3, 4). In §§5, 6, and 7 baroclinic modes over a strong periodic rough relief are investigated by asymptotic methods. Conclusions are stated in §8.

2. Statement of the problem

Quasi-geostrophic low-frequency oscillations are governed by the well-known equation of conservation of potential vorticity; in the linear and rigid-lid approximations we have (cf. Pedlosky 1979):

$$\frac{\partial}{\partial t} \left[\Delta p + \frac{\partial}{\partial z} \left(\frac{f_0^2}{N^2} \frac{\partial p}{\partial z} \right) \right] + \beta \frac{\partial p}{\partial x} = 0. \quad (2.1a)$$

Here p is pressure, t time, x , y , and z the eastward, northward, and vertical coordinates, respectively; and $N = N(z)$ is the buoyancy frequency. The pressure p satisfies the

boundary conditions at the ocean surface:

$$\frac{\partial^2 p}{\partial z \partial t} = 0 \quad \text{at } z = 0, \quad (2.1b)$$

and at its bottom:

$$\frac{\partial^2 p}{\partial z \partial t} = \frac{N^2}{f_0} \left(\frac{\partial p}{\partial y} \frac{\partial h}{\partial x} - \frac{\partial p}{\partial x} \frac{\partial h}{\partial y} \right) \quad \text{at } z = -H. \quad (2.1c)$$

The total ocean depth is assumed to be equal to $h_t = -H + b(x, y)$, where H is the mean depth, and for the depth perturbation we have $b \ll H$.

Let the bottom topography be corrugated so that

$$b = b(y) \quad (2.2)$$

and let the motion depend harmonically on x and t (cf. Part 1):

$$p = \bar{p}(y, z) e^{i(kx - \sigma t)}. \quad (2.3)$$

Here k is the eastward wavenumber and σ is the frequency. From (2.1) we obtain the following problem for the amplitude \bar{p} :

$$\frac{\partial^2 \bar{p}}{\partial y^2} + \frac{\partial}{\partial z} \left(\frac{f_0^2}{N^2} \frac{\partial \bar{p}}{\partial z} \right) - \left(k^2 + \frac{k\beta}{\sigma} \right) \bar{p} = 0, \quad (2.4a)$$

$$\frac{\partial \bar{p}}{\partial z} = 0, \quad z = 0, \quad (2.4b)$$

$$\frac{\partial \bar{p}}{\partial z} = \frac{N^2 k}{\sigma f_0} \frac{dh}{dy} \bar{p}, \quad z = -H. \quad (2.4c)$$

It is convenient to rewrite (2.4) in non-dimensional form using the following dimensionless variables and parameters:

$$\left. \begin{aligned} \hat{y} &= \frac{y}{L_b}, & \hat{z} &= \frac{z}{H}, & b &= \Delta h \hat{b}(\hat{y}), & \delta &= \frac{\Delta h}{H}, \\ \hat{k} &= k L_b, & \hat{\sigma} &= \frac{\sigma}{f_0}, & \hat{\beta} &= \frac{\beta L_b}{f_0}, & n(z) &= \frac{N(z)}{N_0}, \\ \hat{p} &= \frac{\bar{p}}{P}, & \alpha &= \frac{L_i}{L_b}, & L_i &= \frac{H N_0}{f_0}, \end{aligned} \right\} \quad (2.5)$$

where N_0 and P are the buoyancy-frequency and pressure scales.

Writing (2.4) in non-dimensional form we have

$$\frac{\partial^2 \hat{p}}{\partial \hat{y}^2} + \alpha^{-2} \frac{\partial}{\partial \hat{z}} \left(\frac{1}{n^2} \frac{\partial \hat{p}}{\partial \hat{z}} \right) - \left(\hat{k}^2 + \frac{\hat{k} \hat{\beta}}{\hat{\sigma}} \right) \hat{p} = 0, \quad (2.6a)$$

$$\frac{\partial \hat{p}}{\partial \hat{z}} = 0, \quad \hat{z} = 0, \quad (2.6b)$$

$$\frac{\partial \hat{p}}{\partial \hat{z}} = \frac{\alpha^2 \hat{k} \delta}{\hat{\sigma}} n^2 \hat{b}' \hat{p}, \quad \hat{z} = -1, \quad (2.6c)$$

where the prime denotes the differentiation with respect to \hat{y} .

Our task is to investigate the eigenvalue problem (2.6a–c), i.e. to find the eigenvalues \hat{k} , $\hat{\sigma}$ for which bounded solutions to (2.6a–c) exist with given α , $\hat{\beta}$, and δ and to study the properties of the eigenfunctions.

The parameters (2.5) satisfy some conditions. Since quasi-geostrophic motion is considered, the non-dimensional frequency is small:

$$\hat{\sigma} = \sigma/f_0 \ll 1. \quad (2.7a)$$

The topography scale L_b is assumed to be no greater than 50 km, and therefore we have

$$\hat{\beta} = \beta L_b/f_0 = O(0.01), \quad (2.7b)$$

$$\alpha \gtrsim 1. \quad (2.7c)$$

The typical height of the bottom inhomogeneities is assumed to be much smaller than the mean depth H , i.e.

$$\delta = \frac{\Delta h}{H} \ll 1. \quad (2.7d)$$

Finally, we will consider the case of a rough bottom topography, i.e.

$$\hat{k} \sim \frac{L_b}{L} \ll 1. \quad (2.7e)$$

To simplify the notation, in what follows we drop the ‘hat’ over the non-dimensional parameters \hat{k} , $\hat{\sigma}$, $\hat{\beta}$, \hat{y} , and \hat{b} .

3. Heuristic asymptotic theory

The relationships (1.1) adopted in the majority of the above-mentioned papers can be written as

$$\delta \sim \sigma \sim k. \quad (3.1)$$

The simplifying constraint (3.1) makes it impossible to study some important effects, in particular the case of a strong relief where (1.3) holds. At the same time, problem (2.6) for arbitrary relationships among the parameters δ , σ , k , α , and β is too complicated. Therefore we first find a ‘heuristic’ asymptotic solution to system (2.6a–c) for almost arbitrary δ , σ , k , and α using the approach developed by Reznik (1986), and in Part 1. After that, taking account of this solution, we fix the most interesting relationships between δ , σ , k , and α and carry out a more rigorous asymptotic analysis of (2.6) (cf. Part 1).

Thus, the solution is sought in the form

$$p = \bar{p}(Y, z) + \tilde{p}(y, Y, z), \quad (3.2)$$

where $Y = ky$ is a slow coordinate. The term $\bar{p}(Y, z)$ in (3.2) describes a large-scale wave component and $\tilde{p}(y, Y, z)$ corresponds to the small-scale component generated by the interaction of the large-scale component with the rough relief. It is assumed that the component \tilde{p} and its derivatives with respect to z have zero mean value, i.e.

$$\left\langle \frac{\partial^n \tilde{p}}{\partial z^n} \right\rangle = 0, \quad n = 0, 1, 2, \dots \quad (3.3)$$

The averaging in (3.3) is carried out with respect to the ‘fast’ coordinate y :

$$\langle a \rangle = \lim_{L \rightarrow \infty} \frac{1}{2L} \int_{-L}^L a(y) dy. \quad (3.4)$$

Another assumption implies that \bar{p} and \tilde{p} are ‘smooth’ functions of y , Y , and z .

The smoothness of a function $f(y, Y, z)$ means that its derivatives with respect to y , Y , and z are of the order of the function itself, i.e.

$$\frac{\partial^{m+n+k} f}{\partial y^m \partial Y^n \partial z^k} = O(f), \quad m = 0, 1, 2, \dots, \quad n = 0, 1, 2, \dots, \quad k = 0, 1, 2, \dots, \quad (3.5)$$

regardless of the relationships among δ , σ , k , and α .

We now substitute (3.2) into (2.6) and average the resulting equations with respect to y . Taking into account (3.3) we arrive at a set of equations for the large-scale component:

$$k^2 \bar{p}_{YY} + \alpha^{-2} \frac{\partial}{\partial z} \left(\frac{1}{n^2} \frac{\partial \bar{p}}{\partial z} \right) - \left(k^2 + \frac{k\beta}{\sigma} \right) \bar{p} = 0, \quad (3.6a)$$

$$\frac{\partial \bar{p}}{\partial z} = 0, \quad z = 0, \quad (3.6b)$$

$$\frac{\partial \bar{p}}{\partial z} = s \langle b' \bar{p} \rangle, \quad z = -1, \quad (3.6c)$$

where $s = \alpha^2 k \delta n^2 (-1) / \sigma$. Subtraction of (3.6a-c) from (2.6a-c) yields for the small-scale component:

$$\frac{\partial^2 \tilde{p}}{\partial y^2} + \alpha^{-2} \frac{\partial}{\partial z} \left(\frac{1}{n^2} \frac{\partial \tilde{p}}{\partial z} \right) = 0, \quad (3.7a)$$

$$\frac{\partial \tilde{p}}{\partial z} = 0, \quad z = 0, \quad (3.7b)$$

$$\frac{\partial \tilde{p}}{\partial z} = s \langle b' \bar{p} + b' \tilde{p} - \langle b' \tilde{p} \rangle \rangle, \quad z = -1. \quad (3.7c)$$

In view of (2.7c) and the inequality

$$\frac{\beta k}{\sigma} \ll 1, \quad (3.8)$$

which follows from (2.7b) when writing (3.7) we neglect the small terms.

Let the small-scale component be smaller than the large-scale one:

$$\tilde{p} \ll \bar{p} \quad (3.9)$$

(we will verify this assumption *a posteriori*). Then the boundary condition (3.7c) is simplified to

$$\frac{\partial \tilde{p}}{\partial z} = s b' \bar{p}, \quad z = -1. \quad (3.10)$$

The simplified condition (3.10) together with (3.7a, b) allows the small-scale component \tilde{p} to be expressed in terms of the large-scale component \bar{p} and the problem (3.6) for \bar{p} to be closed.

We consider the case when the depth perturbation $b(y)$ is represented as a superposition of a finite number of harmonics in the form

$$b = \sum_{m=-M}^{m=M} b_m e^{i l_m y}, \quad (3.11)$$

where $|l_m| \gtrsim 1$, $l_m = -l_{-m}$, $b_m = b_{-m}^*$, and M is finite (the asterisk denotes the complex conjugate). The solution to the problem (3.7a, b), (3.10), (3.11) can be written in the

form

$$\tilde{p} = i s \bar{p}(-1) \sum_{m=-M}^{m=M} l_m b_m \tilde{p}_m(z) e^{i l_m y}, \quad (3.12)$$

where the coefficients $\tilde{p}_m(z)$ are solutions to

$$\frac{d}{dz} \left(\frac{1}{n^2} \frac{d\tilde{p}_m}{dz} \right) - \alpha^2 l_m^2 \tilde{p}_m = 0, \quad (3.13a)$$

$$\frac{d\tilde{p}_m}{dz} = 0, \quad z = 0, \quad (3.13b)$$

$$\frac{d\tilde{p}_m}{dz} = 1, \quad z = -1. \quad (3.13c)$$

Substituting (3.12) into (3.6c) we obtain

$$\frac{\partial \bar{p}}{\partial z} = -s^2 D \bar{p}, \quad z = -1, \quad (3.14)$$

where D is a positive coefficient:

$$D = \sum_{m=-M}^{m=M} l_m^2 |b_m|^2 |\tilde{p}_m(-1)|. \quad (3.15)$$

When deriving (3.15) we use the relation

$$\tilde{p}_m(-1) = -n^2(-1) \int_{-1}^0 \left[\frac{1}{n^2} \left(\frac{d\tilde{p}_m}{dz} \right)^2 + \alpha^2 l_m^2 \tilde{p}_m^2 \right] dz < 0, \quad (3.16)$$

which is readily implied by (3.13).

Equation (3.6a) and the boundary conditions (3.6b) and (3.14) form a closed problem for the large-scale component \bar{p} . Knowing \bar{p} we can calculate the small-scale component \tilde{p} by formula (3.12). The problem is simplified in the case of a constant buoyancy frequency ($n(z) = 1$). The functions \tilde{p}_m are readily found from (3.13):

$$\tilde{p}_m = -\frac{\cosh \alpha l_m z}{\alpha l_m \sinh \alpha l_m}. \quad (3.17)$$

Accordingly, the coefficient D and function \tilde{p} take the form

$$D = \frac{1}{\alpha} \sum_{m=-M}^{m=M} l_m |b_m|^2 \coth \alpha l_m, \quad (3.18)$$

$$\tilde{p} = -i \bar{p}(-1) \frac{\alpha k \delta}{\sigma} \sum_{m=-M}^{m=M} \frac{\cosh \alpha l_m z}{\sinh \alpha l_m} b_m e^{i l_m y}. \quad (3.19)$$

The large-scale component \bar{p} is sought in the form of a harmonic wave (cf. Reznik & Tsybaneva 1999)

$$\bar{p} = p_0(z) e^{i \bar{l} Y}, \quad (3.20)$$

where the northward wavenumber \bar{l} is assumed to be of the order of 1. By virtue of (3.6a, b), the amplitude $p_0(z)$ is given by the formula

$$p_0 = A \cosh \left(\alpha z \left(\kappa^2 + \frac{k\beta}{\sigma} \right)^{1/2} \right), \quad (3.21a)$$

where $\boldsymbol{\kappa} = (k, k\bar{l})$ is the wave vector and A is an arbitrary constant. Substituting (3.21a) into the bottom boundary condition (3.14) we obtain the dispersion relation in the form:

$$\sigma^2 \alpha \left(\kappa^2 + \frac{k\beta}{\sigma} \right)^{1/2} \tanh \left(\alpha \left(\kappa^2 + \frac{k\beta}{\sigma} \right)^{1/2} \right) = \alpha^4 k^2 \delta^2 D. \quad (3.21b)$$

In view of (3.19), the applicability condition (3.9) for the theory under consideration can be represented as

$$B = \frac{\alpha k \delta}{\sigma} \ll 1. \quad (3.22)$$

Let L be of the order of the Rossby scale L_i . In this case we have $L_b \ll L_i$, and therefore $\alpha \gg 1$, and, consequently, the expression for the small-scale component (3.19) can be approximated by

$$\tilde{p} = -ip_0(-1)B \sum_{m=-M}^{m=M} b_m \operatorname{sgn} l_m e^{il_m y - \alpha |l_m| (1+z)} + O(e^{-\alpha |l_m|}). \quad (3.23)$$

Thus, if the relief scale L_b is less than the Rossby scale L_i , then the small-scale component is confined to a thin near-bottom layer $(L_b/L_i)H$ thick. Recall (for more details see Part 1) that in the two-layer model the analogous small-scale component is concentrated in the lower layer when $L_b \ll L_i$.

4. Analysis of the dispersion relation

(a) *Constant depth.* Let the ocean have a constant depth, i.e. $\delta = 0$ in (3.21b). In this case (3.21b) has non-trivial solutions only if k is negative and

$$\kappa^2 + \frac{k\beta}{\sigma} < 0; \quad (4.1)$$

the frequency σ is always assumed to be positive. The dispersion relation (3.21b) takes the form

$$\tan \left(\alpha \left(-\kappa^2 - \frac{k\beta}{\sigma} \right)^{1/2} \right) = 0, \quad (4.2)$$

whence we obtain a countable set of the roots:

$$\sigma_n^{(0)} = -\frac{k\beta}{\kappa^2 + \alpha^{-2} \pi^2 n^2}, \quad n = 0, 1, \dots \quad (4.3)$$

It is clear that (4.3) determines the dispersion relations for the barotropic ($n = 0$) and baroclinic ($n \geq 1$) Rossby waves in a stratified ocean of constant depth.

(b) *Topographic waves.* Let $\beta = 0$, i.e. let the β -effect be neglected. It follows from (3.21b) that

$$\sigma_{ip}^{(0)} = \alpha^2 \delta (D)^{1/2} |k| \left(\frac{\coth \alpha \kappa}{\alpha \kappa} \right)^{1/2}. \quad (4.4)$$

Thus, the corrugated relief supports propagating waves even without β -effect (cf. Rhines & Bretherton 1973; Part 1). Using (3.19), (3.18), and (4.4) one can readily show that $B \ll 1$, and thus the assumption (3.9) of our asymptotic analysis is fulfilled.

In the long-wave limit, $L \gg L_i$, we have $\alpha \kappa \ll 1$, and the large-scale component \bar{p} is practically barotropic (see (3.21a)). If $L = O(L_i)$, then we have $\alpha \kappa = O(1)$, and \bar{p} gradually increases with increasing z . These characteristics agree with the behaviour

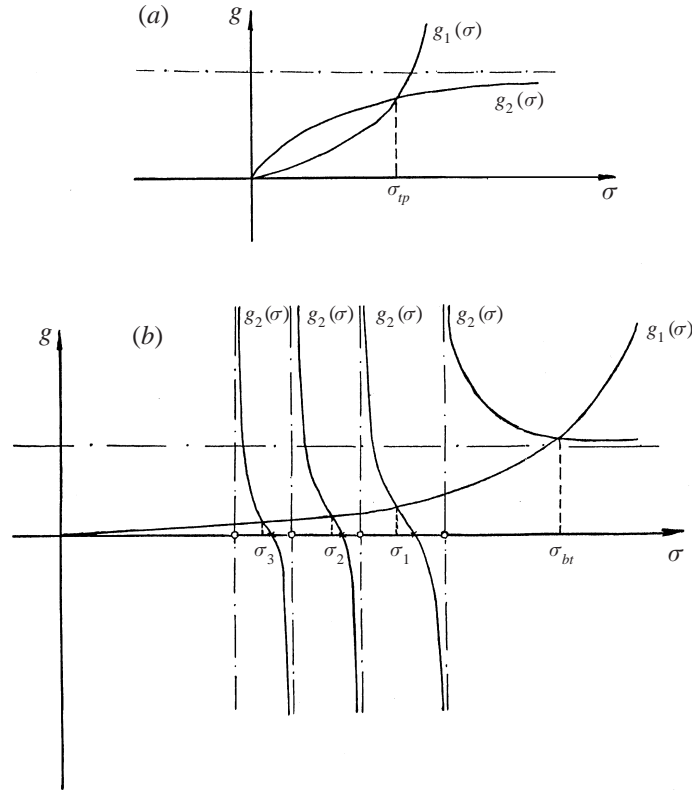


FIGURE 1. Graphical solution of the dispersion equation (3.21b). Dash-dot line represents vertical and horizontal asymptotes of the function $g_2(\sigma)$. (a) $k > 0$. The solution represents the topographic mode σ_{ip} . (b) $k < 0$. Countable number of solutions represent the barotropic σ_{bt} and the baroclinic σ_n , $n = 1, 2, \dots$ modes. Asterisks and circles denote the zeros σ_n^* , $n = 1, 2, \dots$ of the function $g_2(\sigma)$ and the intersection points $\sigma_n^{(0)}$, $n = 0, 1, \dots$ of the vertical asymptotes with the σ -axis respectively.

of topographic waves in the two-layer model (Part 1). At the same time the waves under study essentially differ from barotropic and two-layer topographic waves. The frequencies of these topographic waves are of the order of the relative height of the relief inhomogeneity, i.e.

$$\sigma = O(\delta). \tag{4.5}$$

In a continuously stratified ocean the topographic wave frequency essentially depends on the stratification because the parameter α in (4.4) is proportional to N_0 .

(c) *General case.* To analyse (3.21b) it is convenient to fix all parameters except σ . We need to find the points of intersection for the graphs of the functions

$$g_1(\sigma) = \frac{\sigma^2}{\alpha^4 k^2 \delta^2 D}, \quad g_2(\sigma) = \frac{\coth(\alpha(\kappa^2 + \beta k/\sigma)^{1/2})}{\alpha(\kappa^2 + \beta k/\sigma)^{1/2}}. \tag{4.6}$$

These graphs are shown in figures 1(a) and 1(b) for $k > 0$ and $k < 0$, respectively. The intersection points of the vertical asymptotes of $g_2(\sigma)$ with the σ -axis are $\sigma_n^{(0)}$ (see (4.3)) and

$$\sigma_n^* = -\frac{\beta k}{\kappa^2 + \alpha^{-2} \pi^2 (n - 1/2)^2}, \quad n = 1, 2, \dots, \tag{4.7}$$

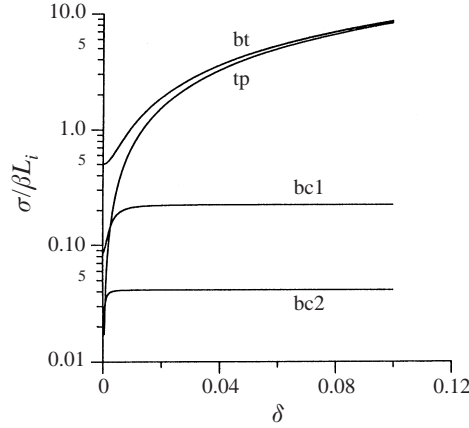


FIGURE 2. Dependence of the mode frequencies on the relative height δ of the topography for given wavenumbers k, l . $|k| = l = 0.01 \text{ km}^{-1}$, $k > 0$ for the topographic mode and $k < 0$ for the baroclinic and barotropic modes. The following dimensional parameters are chosen $\beta = 2 \times 10^{-8} \text{ km}^{-1} \text{ s}^{-1}$, $f_0 = 6 \times 10^{-5} \text{ s}^{-1}$, $L_i = 100 \text{ km}$, $L_b = 10 \text{ km}$; in (3.21b) $\alpha = 10$, $D = 10$. The curves bt, tp, bc1, and bc2 correspond to the barotropic, topographic, 1st and 2nd baroclinic modes, respectively.

are the zeros of $g_2(\sigma)$. It is seen from figure 1 that the following set of wave modes exists here:

- (i) topographic mode ($k > 0$) with frequency σ_{tp} :

$$0 < \sigma_{tp} \leq \sigma_{tp}^{(0)}; \quad (4.8a)$$

- (ii) barotropic mode ($k < 0$) with frequency σ_{bt} :

$$\sigma_0^{(0)} \leq \sigma_{bt} < \infty; \quad (4.8b)$$

- (iii) baroclinic modes ($k < 0$) with frequencies σ_n :

$$\sigma_n^{(0)} \leq \sigma_n \leq \sigma_n^*, \quad n = 1, 2, \dots \quad (4.8c)$$

We now examine the effect of the height of the relief inhomogeneity on these modes; to do this we vary δ as the other parameters remain fixed. One can readily see that for $\delta \rightarrow 0$ the coefficient of the parabola $g_1(\sigma)$ tends to infinity, and therefore the topographic mode degenerates ($\sigma_{tp} \rightarrow 0$), whereas the barotropic (σ_{bt}) and baroclinic (σ_n , $n = 1, 2, \dots$) modes are transformed into the corresponding Rossby modes in the ocean of constant depth: $\sigma_{bt} \rightarrow \sigma_0^{(0)}$, $p_{bt} \rightarrow \text{const}$; $\sigma_n \rightarrow \sigma_n^{(0)}$, and

$$p_{0n} \rightarrow p_{0n}^{(0)} = A \cos(\pi n z), \quad n = 1, 2, \dots, \quad (4.9a)$$

as $\delta \rightarrow 0$. It is this property of the modes under consideration that accounts for their names (cf. Part 1).

Conversely, with increasing δ the coefficient of the parabola $g_1(\sigma)$ decreases, and the frequencies σ_{tp} and σ_{bt} increase, tending to the frequency of the pure topographic mode (4.4). The behaviour of the baroclinic modes is more non-trivial. Their frequencies σ_n also somewhat increase with increasing δ but they tend to σ_n^* and therefore the baroclinic modes remain low-frequency oscillations over the strong relief. All these characteristics are clearly seen in figure 2.

The spatial structure of the baroclinic modes significantly changes with increasing height of the relief inhomogeneity. For the vertical profile p_{0n} of the large-scale

baroclinic component we have

$$p_{0n} \rightarrow p_{0n}^* = A \cos\left(\pi\left(n - \frac{1}{2}\right)z\right), \quad n = 1, 2, \dots, \quad (4.9b)$$

as δ increases. The comparison of (4.9a) and (4.9b) shows that the large-scale component \bar{p} decreases near the bottom as δ increases. Accordingly, the small-scale component \tilde{p} also reduces with decreasing $p_{0n}(-1)$ (see (3.19)).

Thus, as in the case of the two-layer model (Part 1), the effect of ‘displacement’ manifests itself. As the height of the relief inhomogeneity increases the large-scale baroclinic motion in the bottom layer decreases, and, in turn, this causes a decrease in the small-scale component. The resulting effect is that the strong relief displaces the baroclinic motion from the near-bottom layer.

For a more accurate analysis we rewrite the dispersion relation (3.21b) as follows:

$$\gamma^2 \tilde{\sigma}^2 = \frac{\coth\left(\alpha\kappa(1 + \tilde{\sigma}^{-1} \operatorname{sgn} k)^{1/2}\right)}{\alpha\kappa(1 + \tilde{\sigma}^{-1} \operatorname{sgn} k)^{1/2}}, \quad (4.10)$$

where

$$\gamma^2 = \frac{\beta^2}{\alpha^4 \kappa^4 \delta^2 D}, \quad \tilde{\sigma} = \frac{\kappa^2 \sigma}{\beta |k|}. \quad (4.11)$$

The parameter $\tilde{\sigma}$ is equal to the ratio of the oscillation frequency to the barotropic Rossby wave frequency.

We now examine the important case where the scale L has the same order of magnitude as the Rossby scale L_i , i.e.

$$\alpha\kappa \simeq \frac{L_i}{L} = O(1), \quad \alpha = \frac{L_i}{L_b} \gg 1. \quad (4.12)$$

Let us investigate (4.10) for different values of the parameter γ , which, under the constraint (4.12), is

$$\gamma = O\left(\frac{\beta\alpha^{1/2}}{\delta}\right). \quad (4.13)$$

The results of the analysis of (4.10) are presented in table 1 (cf. table 1 in Part 1). As is seen from table 1, the effect of the bottom relief is weak if $\gamma \gg 1$ and strong for $\gamma \ll 1$.

This classification of the relief differs significantly from that in the two-layer case. In the two-layer model (Part 1) the efficiency of the topography for $L \simeq L_i$ is determined by the parameter $\Delta = \delta/\alpha\beta$ characterizing the relative contributions of the topography and β -effect. In the case under consideration the effect of the relief depends on the parameter $\gamma = 1/(\Delta\alpha^{1/2}) \ll \Delta^{-1}$, i.e. the relief efficiency is significantly higher than in the two-layer case (for example, $\Delta \simeq 1$ corresponds to a moderate relief in the two-layer case and to a strong relief for $N = \text{const}$ because $\gamma \ll 1$ for $\Delta = 1$). However, note that for the actual profile $N(z)$ this distinction from the two-layer model can be softened considerably because the buoyancy frequency in the abyssal region is small compared to the main thermocline. Accordingly, the parameter s in (3.10), which, ultimately, determines the relief efficiency, can be very small.

As is seen from table 1, the condition (3.22) of applicability for the presented dispersion relations holds well in all the cases except for the baroclinic modes over a strong relief for which the applicability condition can be rewritten in the following

	Weak relief ($\gamma \gg 1$)	Strong relief ($\gamma \ll 1$)
Topographic mode ($k > 0$)	$\sigma = \frac{\alpha^2 D^{2/3} \delta^{4/3} k}{\beta^{1/3}}$ $\alpha^{-1} \ll \frac{\delta}{\beta} \ll \alpha^{1/2}$	$\sigma = \sigma_{ip}^{(0)}$ $= \alpha^2 \delta k \left(\frac{D \operatorname{cotanh}(\alpha \kappa)}{\alpha \kappa} \right)^{1/2}$ $1 \ll \alpha^{1/2} \ll \frac{\delta}{\beta}$
Barotropic mode ($k < 0$)	$\sigma = \sigma_0^{(0)} = -\frac{\beta k}{\kappa^2}$ $\frac{\delta}{\beta} \ll \alpha^{1/2}$	$\sigma = \sigma_{ip}^{(0)}$ $= -\alpha^2 \delta k \left(\frac{D \operatorname{cotanh}(\alpha \kappa)}{\alpha \kappa} \right)^{1/2}$ $1 \ll \alpha^{1/2} \ll \frac{\delta}{\beta}$
Baroclinic modes ($k < 0$)	$\sigma = \sigma_n^{(0)}$ $= -\frac{\beta k}{\kappa^2 + \alpha^{-2} \pi^2 n^2}$ $\frac{\delta}{\beta} \ll \min \left\{ \alpha^{1/2}, \frac{\alpha}{\pi^2 n^2} \right\},$ $n = 1, 2, \dots$	$\sigma = \sigma_n^*$ $= -\frac{\beta k}{\kappa^2 + \alpha^{-2} \pi^2 (n - \frac{1}{2})^2}$ $\alpha^{1/2} \ll \frac{\delta}{\beta} \ll \frac{\alpha}{\pi^2 (n - \frac{1}{2})^2},$ $n = 1, 2, \dots$

TABLE 1. Characteristics of the oscillation modes.

way:

$$\frac{(L_i L_b)^{1/2}}{a} \ll \delta \ll \frac{L_i}{\pi^2 (n - 1/2)^2 a}, \quad n = 1, 2, \dots, \quad (4.14a)$$

where $a = f_0/\beta$. For typical scales ($L_i = 100$ km and $a = 3000$ km) the inequality (4.14a) gives

$$10^{-2} \ll \delta \ll \frac{3 \times 10^{-3}}{(n - 1/2)^2}, \quad n = 1, 2, \dots \quad (4.14b)$$

As is seen from (4.14b), condition (4.14a) fails even for the first baroclinic mode ($n = 1$).

The lower bound in (4.14a) diminishes with decreasing relief scale L_b (cf. Part 1). When $L_b = 10$ m, the lower bound in (4.14a) is about 3×10^{-4} , and (4.14a) is satisfied crudely for $\delta = 10^{-3}$. An analysis of the baroclinic mode with a physically reasonable scale L_b requires that the constraint (3.22) on the wave parameters be abandoned. An asymptotic analysis of baroclinic waves for $B \sim 1$ is presented in the next Section.

5. Baroclinic modes over strong relief

We now consider again problem (2.6) with $N = \text{const}$, i.e. $n(z) = 1$. The scale L is assumed to be of the order of L_i , and therefore (4.12) holds. We will restrict our consideration to baroclinic modes (which are the most interesting for applications), whose dimensional frequencies are of the order of βL irrespective of the relief height (see table 1). In view of (4.12), the dimensionless frequency σ of this mode is of the

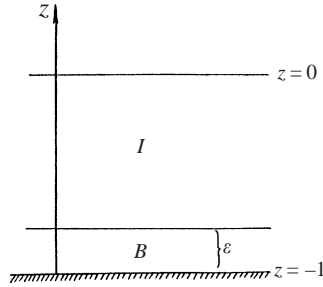


FIGURE 3. A sketch of the near-bottom boundary layer (B) and the interior region (I).

order of $\alpha\beta$, and for the parameter B in (3.22) we have

$$B = \frac{\alpha k \delta}{\sigma} = O\left(\frac{\delta}{\alpha\beta}\right). \tag{5.1}$$

We examine the case of a sufficiently high relief inhomogeneity where

$$\delta \sim \sigma \sim \alpha\beta, \tag{5.2}$$

and therefore, in contrast to §§ 3 and 4,

$$B \sim 1. \tag{5.3}$$

System (2.6) can be rewritten conveniently in the form

$$\frac{\partial^2 p}{\partial y^2} + \varepsilon^2 \frac{\partial^2 p}{\partial z^2} - \varepsilon^2 A p = 0, \tag{5.4a}$$

$$\frac{\partial p}{\partial z} = 0, \quad z = 0, \tag{5.4b}$$

$$\frac{\partial p}{\partial z} = \frac{B}{\varepsilon} b' p, \quad z = -1, \tag{5.4c}$$

where

$$\varepsilon = \alpha^{-1} \ll 1, \quad A = \alpha^2 \left(k^2 + \frac{k\beta}{\sigma} \right) \sim 1. \tag{5.5}$$

The solution derived in § 3 suggests that a boundary layer of thickness ε is formed near the bottom (region B in figure 3); in the interior (region I) the pressure p depends ‘smoothly’ on z . The problem also involves various horizontal scales, and therefore it is reasonable to use the method of multiple scales here. Accordingly, the solution in region I is sought in the form

$$p = p_I = p_0(y, z, Y_1, Y_2, \dots) + \varepsilon p_1(y, z, Y_1, Y_2, \dots) + \dots, \tag{5.6a}$$

and in region B we write

$$p = p_I + \hat{p}_0(y, \zeta, Y_1, Y_2, \dots) + \varepsilon \hat{p}_1(y, \zeta, Y_1, Y_2, \dots) + \dots. \tag{5.6b}$$

Here $Y_m = \varepsilon^m y$, $m = 1, 2, \dots$ are slow variables, $\zeta = (1 + z)/\varepsilon$ is the stretched boundary-layer variable, and

$$\hat{p}_k \rightarrow 0, \quad \zeta \rightarrow +\infty, \quad k = 0, 1, 2, \dots. \tag{5.7}$$

In addition, the functions p_k , \hat{p}_k , $k = 0, 1, \dots$ must be bounded in both the fast variable y and the slow variables Y_m , $m = 1, 2, \dots$.

Substituting (5.6a) into (5.4a) we obtain

$$\frac{\partial^2 p_0}{\partial y^2} = 0, \quad (5.8a)$$

$$\frac{\partial^2 p_1}{\partial y^2} + 2 \frac{\partial^2 p_0}{\partial y \partial Y_1} = 0, \quad (5.8b)$$

$$\frac{\partial^2 p_2}{\partial y^2} + 2 \frac{\partial^2 p_1}{\partial y \partial Y_1} + 2 \frac{\partial^2 p_0}{\partial y \partial Y_2} + M p_0 = 0, \quad (5.8c)$$

$$\frac{\partial^2 p_3}{\partial y^2} + 2 \frac{\partial^2 p_2}{\partial y \partial Y_1} + 2 \frac{\partial^2 p_1}{\partial y \partial Y_2} + 2 \frac{\partial^2 p_0}{\partial y \partial Y_3} + 2 \frac{\partial^2 p_0}{\partial Y_1 \partial Y_2} + M p_1 = 0, \quad (5.8d)$$

where

$$M = \frac{\partial^2}{\partial Y_1^2} + \frac{\partial^2}{\partial z^2} - A. \quad (5.8e)$$

An analysis of equations (5.8) shows that the boundedness for $y \rightarrow \pm\infty$ implies that p_k does not depend on y , i.e.

$$p_k = p_k(z, Y_1, Y_2, \dots), \quad k = 0, 1, \dots \quad (5.9)$$

Taking (5.9) into account we obtain from (5.8) the relations

$$M p_0 = 0, \quad (5.10a)$$

$$M p_1 = -2 \frac{\partial^2 p_0}{\partial Y_1 \partial Y_2}, \quad (5.10b)$$

etc. Substituting (5.6a) into (5.4b) and using (5.7) we derive the following boundary conditions for p_k , $k = 0, 1, \dots$ at the ocean surface:

$$\frac{\partial p_k}{\partial z} = 0, \quad z = 0, \quad k = 0, 1, \dots \quad (5.11)$$

Similarly, substituting (5.6b) into (5.4a, c) we obtain the equations

$$\Delta \hat{p}_0 = 0, \quad (5.12a)$$

$$\Delta \hat{p}_1 = -2 \frac{\partial^2 \hat{p}_0}{\partial y \partial Y_1}, \quad (5.12b)$$

$$\Delta \hat{p}_2 = -2 \frac{\partial^2 \hat{p}_1}{\partial y \partial Y_1} - 2 \frac{\partial^2 \hat{p}_0}{\partial y \partial Y_2} - \frac{\partial^2 \hat{p}_0}{\partial Y_1^2} + A \hat{p}_0 \quad (5.12c)$$

and the boundary conditions at the bottom ($z = -1$):

$$\frac{\partial \hat{p}_0}{\partial \zeta} = B b'(p_0 + \hat{p}_0), \quad (5.13a)$$

$$\frac{\partial \hat{p}_1}{\partial \zeta} + \frac{\partial p_0}{\partial z} = B b'(p_1 + \hat{p}_1), \quad (5.13b)$$

$$\frac{\partial \hat{p}_2}{\partial \zeta} + \frac{\partial p_1}{\partial z} = B b'(p_2 + \hat{p}_2), \quad (5.13c)$$

where

$$\Delta = \frac{\partial^2}{\partial y^2} + \frac{\partial^2}{\partial \zeta^2}.$$

The scheme of the solution is the following. Given $p_k(-1)$ and $(\partial p_k / \partial z)(-1)$, the equations for \hat{p}_k , $k = 0, 1, \dots$, are analysed (each of the problems is given by the corresponding equation (5.12) and boundary conditions (5.7), (5.13)). The solvability conditions of the equations for \hat{p}_k determine the relationships between $p_k(-1)$ and $(\partial p_k / \partial z)(-1)$, i.e. the boundary conditions for p_k at $z = -1$. Knowing these conditions and using (5.10), (5.11) one can determine the functions p_k and the dispersion relation.

Realization of this algorithm is a too complicated problem even for the almost periodic relief (3.11), and we examine here the sinusoidal topography

$$b = \sin y. \quad (5.14)$$

The solution to (5.12a), (5.13a), (5.7) is sought in the form of a series

$$\hat{p}_0 = \sum_{n=1}^{\infty} a_n^{(0)} \cos ny e^{-n\zeta}, \quad (5.15)$$

satisfying (5.7) and (5.12a). Substitution of (5.15) into (5.13a) gives the following relations for $a_n^{(0)}$:

$$a_1^{(0)} = 0, \quad a_2^{(0)} = -2p_0(-1), \quad (5.16a, b)$$

$$a_{n+1}^{(0)} + a_{n-1}^{(0)} = -\frac{2n}{B} a_n^{(0)}, \quad n = 2, 3, \dots \quad (5.16c)$$

Relations (5.16c) can be regarded as a second-order finite-difference equation for the coefficient $a_n^{(0)}$, and (5.16a, b) are the 'initial' conditions for this equation. The general solution to (5.16) can be written as (cf. Gradshteyn & Ryzhik 1965)

$$a_n^{(0)} = (-1)^n [C_1^{(0)} J_n(B) + C_2^{(0)} Y_n(B)], \quad n = 1, 2, \dots, \quad (5.17)$$

where $J_n(B)$, $Y_n(B)$ are the Bessel functions of the first and the second kind, respectively and $C_1^{(0)}$ and $C_2^{(0)}$ are some arbitrary constants. Substituting (5.17) into (5.16a, b) we obtain the equations for $C_1^{(0)}$, $C_2^{(0)}$:

$$C_1^{(0)} J_1(B) + C_2^{(0)} Y_1(B) = 0, \quad (5.18a)$$

$$C_1^{(0)} J_2(B) + C_2^{(0)} Y_2(B) = -2p_0(-1). \quad (5.18b)$$

The functions $J_n(B)$ and $Y_n(B)$ behave in the following way as $n \rightarrow \infty$ (cf. Gradshteyn & Ryzhik 1965):

$$J_n(B) = O\left(n^{-1/2} \left(\frac{2n}{eB}\right)^{-n}\right), \quad Y_n(B) = O\left(n^{-1/2} \left(\frac{2n}{eB}\right)^n\right), \quad (5.19)$$

and therefore series (5.15) converges only if

$$C_2^{(0)} = 0. \quad (5.20)$$

Equations (5.18a, b) take the form

$$C_1^{(0)} J_1(B) = 0, \quad C_1^{(0)} J_2(B) = -2p_0(-1). \quad (5.21)$$

We first assume that

$$B \neq \pm j_{1,s}, \quad (5.22)$$

where $j_{1,s}$, $s = 1, 2, \dots$ are the positive zeros of the function $J_1(x)$. Under this condition we have $J_1(B) \neq 0$, and it follows from (5.21) that

$$C_1^{(0)} = 0, \quad p_0(-1) = 0. \quad (5.23a, b)$$

By virtue of (5.20), (5.23a),

$$\hat{p}_0 = 0, \quad (5.24)$$

i.e. expansion (5.6b) for the small-scale bottom boundary layer component begins with a term of the order of ε . At the same time, conditions (5.11) and (5.23b) together with equation (5.10a) determine completely the problem for the large-scale component p_0 . Let p_0 depend harmonically on Y_1 (cf.(3.20)):

$$p_0 = \bar{p}_0(z, Y_2, Y_3, \dots) e^{i l_1 Y_1}, \quad l_1 \sim 1. \quad (5.25)$$

Then it follows from (5.10a), (5.11), (5.23b), and (5.5) that a countable number of baroclinic modes with dispersion relations

$$\sigma = \sigma_n^* = -\frac{k\beta}{\kappa^2 + \alpha^{-2}\pi^2(n-1/2)^2}, \quad n = 1, 2, \dots, \quad (5.26a)$$

and eigenfunctions

$$p_0 = p_{0n}^* = Q_0(Y_2, Y_3, \dots) \cos(\pi(n-1/2)z) e^{i l_1 Y_1}, \quad n = 1, 2, \dots, \quad (5.26b)$$

correspond to the wave vector $\kappa = (k, l_1/\alpha)$. Thus, in the case of higher relief inhomogeneity when we have $B \sim 1$ (unlike $B \ll 1$ in §4) the effect of displacement of motion from the near-bottom layer also takes place.

The solution for \hat{p}_1 is sought in the form of a series similar to (5.15):

$$\hat{p}_1 = \sum_{n=1}^{\infty} a_n^{(1)} \cos ny e^{-n\zeta}, \quad (5.27)$$

which, in view of (5.24), satisfies (5.12b). It follows from (5.13b) that the coefficients $a_n^{(1)}$ obey the relations

$$a_1^{(1)} = \frac{2}{B} p_{0z}(-1), \quad a_2^{(1)} = -\frac{4}{B^2} p_{0z}(-1) - 2p_1(-1), \quad (5.28a, b)$$

$$a_{n+1}^{(1)} + a_{n-1}^{(1)} = -\frac{2n}{B} a_n^{(1)}, \quad n = 2, 3, \dots \quad (5.28c)$$

The general solution of (5.28c) has the form (cf. (5.17))

$$a_n^{(1)} = (-1)^n [C_1^{(1)} J_n(B) + C_2^{(1)} Y_n(B)], \quad n = 1, 2, \dots \quad (5.29)$$

Substituting (5.29) into (5.28a, b) with $C_2^{(1)} = 0$ we obtain after some simple algebra the formulas

$$p_1(-1) = -\frac{J_0(B)}{B J_1(B)} p_{0z}(-1), \quad (5.30a)$$

$$a_n^{(1)} = (-1)^{n+1} \frac{2J_n(B)}{B J_1(B)} p_{0z}(-1), \quad n = 1, 2, \dots \quad (5.30b)$$

Formulas (5.30b) determine completely the solution (5.27) for \hat{p}_1 (in view of (5.19) this series converges very rapidly). Relation (5.30a) is a 'missing' boundary condition for p_1 at the bottom making it possible to find p_1 from (5.10b), (5.11), (5.30a) and to determine the Y_2 -dependence of p_0 from the requirement that p_1 be bounded as a function of Y_1 . Evidently, this procedure can be continued to attain any required accuracy.

6. Resonance case

Let condition (5.22) be violated, i.e. let the parameter B coincide with one of the zeros of $J_1(x)$:

$$B = B_0 = \pm j_{1,s}, \quad s = 1, 2, \dots, \quad J_1(B_0) = 0. \quad (6.1)$$

Since B is assumed to be of the order of 1 (see (5.3)), only the case $B_0 = \pm j_{1,1} = \pm 3.83\dots$ is of practical interest. One can readily see that the solution obtained in the preceding Section fails under condition (6.1): the first relation in (5.21) is fulfilled identically, whereas the second one gives

$$C_1^{(0)} = -\frac{2p_0(-1)}{J_2(B_0)} \quad (6.2)$$

(cf. (5.23)). Using (5.17), (6.2), and (5.20) one can write the coefficients $a_n^{(0)}$ in (5.15) as follows:

$$a_n^{(0)} = (-1)^{n+1} \frac{2p_0(-1)}{J_2(B_0)} J_n(B_0), \quad n = 1, 2, \dots \quad (6.3)$$

So, in contrast to the foregoing case, an analysis of the lowest small-scale correction \hat{p}_0 does not permit the boundary condition for p_0 at the bottom to be determined. The solution for p_0 satisfying (5.10a), (5.11) and harmonically depending on Y_1 can be written as

$$p_0 = Q_0(Y_2, Y_3, \dots) \cos(z(-A - l_1^2)^{1/2}) e^{il_1 Y_1}. \quad (6.4)$$

To determine the bottom boundary condition for p_0 we examine the problem (5.12b), (5.7), and (5.13b) for \hat{p}_1 . The solution to (5.12b) is sought in the form of a sum

$$\hat{p}_1 = \hat{p}_{10} + \hat{p}_{11}, \quad (6.5)$$

where

$$\hat{p}_{10} = -\sum_{n=2}^{\infty} \frac{\partial a_n^{(0)}}{\partial Y_1} \zeta \sin(ny) e^{-n\zeta} \quad (6.6a)$$

is a particular solution to (5.12b) and

$$\hat{p}_{11} = \sum_{n=1}^{\infty} (a_n^{(1)} \cos(ny) + d_n^{(1)} \sin(ny)) e^{-n\zeta} \quad (6.6b)$$

is a solution to (5.12b) with a zero right-hand side. Substituting \hat{p}_1 into the bottom condition (5.13b) we obtain a relation determining the coefficients $a_n^{(1)}$, $d_n^{(1)}$ in (6.6b). The system for $a_n^{(1)}$ coincides with (5.28) for $B = B_0$, and therefore the solution for $a_n^{(1)}$ is given by formula (5.29) with $B = B_0$. Relations (5.30) change in the following way:

$$p_{0z}(-1) = 0, \quad (6.7a)$$

$$a_n^{(1)} = (-1)^{n+1} \frac{2J_n(B_0)}{J_2(B_0)} p_1(-1). \quad (6.7b)$$

The system for the coefficients $d_n^{(1)}$ has the form

$$d_1^{(1)} + \frac{B_0}{2} d_2^{(1)} = 0, \quad (6.8a)$$

$$d_{n+1}^{(1)} + d_{n-1}^{(1)} + \frac{2n}{B_0} d_n^{(1)} = -\frac{2}{B_0} \frac{\partial a_n^{(0)}}{\partial Y_1}, \quad n = 2, 3, \dots \quad (6.8b)$$

The solution to (6.8a, b) tending to zero as $n \rightarrow \infty$ is given in the Appendix.

Relation (6.7a) is a ‘missing’ condition for the large-scale component p_0 at the bottom. From (6.4) and (6.7a) we obtain the leading term in the large-scale component

$$p_0 = p_{0n}^{(0)} = Q_0(Y_2, Y_3, \dots) \cos(\pi n z) e^{i l_1 Y_1} \quad (6.9a)$$

and the corresponding dispersion relation

$$\sigma = \sigma_n^{(0)} = -\frac{k\beta}{\kappa^2 + \alpha^{-2}\pi^2 n^2}, \quad n = 0, 1, \dots \quad (6.9b)$$

The frequency σ and the wave vector κ must satisfy, in addition to (6.9b), the condition (6.1), which can be rewritten as

$$\sigma = \sigma_s = -\frac{\alpha\delta k}{j_{1,s}}, \quad s = 1, 2, \dots \quad (6.9c)$$

Thus, with the constraint (6.1) the leading term \hat{p}_0 in the expansion (5.6b) for the small-scale component is non-zero in contrast to the case $B \neq j_{1,s}$ considered in §5. In other words, a kind of resonance arises for $B = j_{1,s}$ when the amplitude of the near-bottom small-scale component increases strongly (it is ε^{-1} times as large as in the non-resonance case $B \neq j_{1,s}$) and the small-scale velocity exceeds the large-scale one in the near-bottom boundary layer. Moreover, in contrast to the non-resonance case, the large-scale component (6.9a) does not vanish when approaching the bottom; on the contrary, it has a local maximum here. Thus, if the frequency σ and the wavenumber k satisfy the constraint (6.9c), then both the small- and large-scale components intensify strongly near the bottom. A similar resonance effect manifesting itself in the intensification of the wave in the lower layer takes place in the two-layer model as well (Part 1).

7. Transient solution

The non-resonance solution constructed in §5 fails when B tends to B_0 because the coefficients $a_n^{(1)}$ in (5.30b) tend to infinity as $B \rightarrow B_0$. To obtain the solution in the transition region between the resonance and non-resonance modes we introduce the stretched variable

$$\xi = \frac{B - B_0}{\varepsilon}. \quad (7.1)$$

The solution coincides with the resonance solution for $\xi = 0$ and tends to the non-resonance one as $\xi \rightarrow \infty$; in the transition region $\xi = O(1)$.

We now write the boundary condition (5.4c) using the parameter ξ :

$$\frac{\partial p}{\partial z} = \left(\frac{B_0}{\varepsilon} + \xi \right) b' p, \quad z = -1, \quad (7.2)$$

and assume the expansions (5.6a, b) to depend on ξ in the transition region. Evidently, when substituting (5.6) into (5.4a, b) and (7.2) only the boundary conditions (5.13) at $z = -1$ ($\zeta = 0$) change:

$$\frac{\partial \hat{p}_0}{\partial \zeta} = B_0 b'(p_0 + \hat{p}_0), \quad (7.3a)$$

$$\frac{\partial \hat{p}_1}{\partial \zeta} + \frac{\partial p_0}{\partial z} = B_0 b'(p_1 + \hat{p}_1) + \xi b'(p_0 + \hat{p}_0), \quad (7.3b)$$

$$\frac{\partial \hat{p}_2}{\partial \zeta} + \frac{\partial p_1}{\partial z} = B_0 b'(p_2 + \hat{p}_2) + \xi b'(p_1 + \hat{p}_1), \quad (7.3c)$$

whereas equations (5.8)–(5.12) remain the same.

The equation and the boundary conditions for \hat{p}_0 are the same as those in § 6, and therefore \hat{p}_0 is given by formulas (5.15), (6.3). The large-scale component p_0 satisfying (5.10a), (5.11) is given by expression (6.4). The boundary condition for p_0 at $z = -1$ is found from an analysis of the function \hat{p}_1 , which has the form (6.5), (6.6a, b). Substituting (6.5) and (6.6) into (7.3) we obtain the following non-homogeneous system for $a_n^{(1)}$:

$$a_1^{(1)} = \frac{2}{B_0} p_{0z}(-1), \quad (7.4a)$$

$$a_2^{(1)} = -\frac{2}{B_0} \left\{ \frac{2}{B_0} p_{0z}(-1) + B_0 p_1(-1) + \xi p_0(-1) + \frac{\xi}{2} a_2^{(0)} \right\}, \quad (7.4b)$$

$$a_{n+1}^{(1)} + a_{n-1}^{(1)} + \frac{2n}{B_0} a_n^{(1)} = \frac{2\xi n}{B_0^2} a_n^{(0)}, \quad n = 2, 3, \dots, \quad (7.4c)$$

where $a_n^{(0)}$ are given by (6.3). For $d_n^{(1)}$ we again have the system (6.8). The general solution to (7.4) is sought in the form

$$a_n^{(1)} = (-1)^n \left\{ C_1^{(1)} J_n(B_0) + C_2^{(1)} Y_n(B_0) + r_n^{(1)} \right\}, \quad n = 1, 2, \dots, \quad (7.5)$$

where $C_1^{(1)}$ and $C_2^{(1)}$ are arbitrary constants and $r_n^{(1)}$ is a particular solution to (7.4c) tending to zero as $n \rightarrow \infty$. The application of the method of variation of parameters results in (see the Appendix)

$$r_n^{(1)} = \frac{4\xi p_0(-1)}{B_0^2 J_2(B_0)} s_n^{(1)}, \quad (7.6a)$$

where

$$s_n^{(1)} = \frac{\pi B_0}{2} \left\{ J_n(B_0) \sum_{k=1}^{n-1} k J_k(B_0) Y_k(B_0) + Y_n(B_0) \sum_{k=n}^{\infty} k J_k^2(B_0) \right\}. \quad (7.6b)$$

It follows from the boundedness of $a_n^{(1)}$ at $n \rightarrow \infty$ that $C_2^{(1)} = 0$. Substituting (7.5) into (7.4a) and (7.4b) we derive the equation

$$p_{0z}(-1) + \frac{2\xi s_1^{(1)}}{B_0 J_2(B_0)} p_0(-1) = 0, \quad (7.7)$$

which is the missing boundary condition for p_0 . Substitution of (6.4) into (7.7) gives the dispersion relation

$$\tan \gamma = \frac{\lambda}{\gamma}, \quad (7.8a)$$

where

$$\lambda = -\frac{2\xi s_1^{(1)}}{B_0 J_2(B_0)}, \quad (7.8b)$$

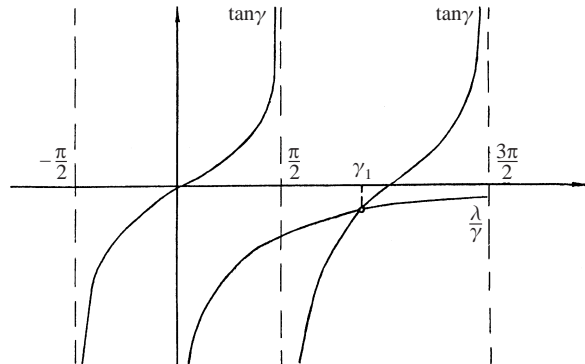
$$\gamma = (-A - l_1^2)^{1/2}. \quad (7.8c)$$

Figure 4 shows that equation (7.8a) has a countable set of non-negative roots:

$$\gamma = \gamma_n(\xi), \quad n = 1, 2, \dots. \quad (7.9a)$$

whence

$$\sigma = \bar{\sigma}_n = -\frac{k\beta}{\kappa^2 + \alpha^{-2}\gamma_n^2}, \quad \kappa^2 = k^2 + \frac{l_1^2}{\alpha^2}, \quad n = 1, 2, \dots. \quad (7.9b)$$

FIGURE 4. Graphical solution of the dispersion equation (7.8a) for $\lambda < 0$.

Formulas (7.8a, b) imply that

$$\gamma_n \rightarrow \pi n, \quad \sigma \rightarrow \sigma_n^{(0)}, \quad \text{at } |\xi| \rightarrow 0, \quad n = 1, 2, \dots, \quad (7.10)$$

i.e. the solution tends to the resonance solution given by (6.9), (5.15), and (6.3) as $\xi \rightarrow 0$ ($B \rightarrow B_0$). However, if $|\xi| \rightarrow \infty$ (B moves away from B_0), then

$$\gamma_n \rightarrow \pi(n - \frac{1}{2}), \quad \sigma \rightarrow \sigma_n^* \quad \text{as } |\xi| \rightarrow \infty, \quad n = 1, 2, \dots, \quad (7.11)$$

i.e. the solution approaches the baroclinic mode over a strong relief defined by (5.24), (5.26a, b).

8. Discussion and conclusions

We have investigated linear Rossby waves in a continuously stratified ocean with a corrugated rough-bottom topography (the isobaths are parallel straight lines). The solution is obtained for the case of a constant buoyancy frequency. The asymptotic theory developed is valid over a wide range of the parameters L_b/L , $\beta L/f_0$, L_b/L_i , and $\Delta h/H$. There exist three types of modes: a topographic mode, a barotropic mode, and a countable set of baroclinic modes. As $\Delta h \rightarrow 0$ the barotropic and baroclinic modes are transformed into the 'usual' barotropic and baroclinic Rossby waves in an ocean of constant depth. The topographic mode degenerates in the limit of constant depth because its frequency tends to zero for $\Delta h \rightarrow 0$.

These modes are in many respects similar to the modes in a two-layer ocean that were investigated in Part 1. For example, the so-called 'screening' effect also occurs in the case under consideration. Here it implies that for $L_b \ll L_i$ the small-scale component of the wave is confined to the near-bottom boundary layer $(L_b/L_i)H$ thick, whereas in the region outside the layer the scale L of motion is always greater than or of the order of L_i (also see McWilliams 1974 and Zhdanov 1987).

The structure and frequencies of the modes substantially depend on the type of mode, the relative height $\Delta h/H$ of the bottom bumps, the wave scale L , the topography scale L_b , and the Rossby scale L_i . Let

$$L \simeq L_i \quad (8.1)$$

in this case the topography effect is determined by the parameter

$$\gamma = \frac{\beta}{\alpha^2 \kappa^2 \delta D} = O\left(\frac{\beta \alpha^{1/2}}{\delta}\right) = O\left(\frac{1}{\Delta \alpha^{1/2}}\right), \quad (8.2)$$

where $\Delta = (\Delta h/H)/(L/a)$ is a measure of relative contributions of the topography and β -effect.

The case $\gamma \gg 1$ corresponds to a weak topography where the barotropic and baroclinic modes are close to those in an ocean of constant depth and the topographic mode degenerates (its dimensionless frequency is $O(\gamma^{-4/3})$ for $\gamma \gg 1$). In the case $\gamma \sim 1$ the topography effect is moderate: the frequencies of the topographic and barotropic modes and of the first baroclinic mode are of the same order, $O(\beta L_i)$. The amplitude of the near-bottom small-scale velocity field is $\alpha^{1/2}$ times as great as that of the large-scale velocity, i.e. an intensification of motion near the bottom takes place for all the modes.

When the topography is strong, i.e. $\gamma \ll 1$, the topographic and barotropic modes are close to a purely topographic mode. With decreasing γ their frequencies increase monotonically and approach the frequency (4.4) of a purely topographic wave as $\gamma \rightarrow 0$ (or, which is the same, $\Delta \rightarrow \infty$). The spatial structure of the modes is qualitatively the same as in the case of a moderate topography.

The behaviour of baroclinic modes for a strong relief is more non-trivial. The frequencies of these modes are always within the range (4.8c), i.e. they do not exceed $O(\beta L_i)$ irrespective of the magnitude of γ . At the same time, the spatial structure of the modes depends essentially on γ . With decreasing γ the large-scale component decreases near the bottom together with the small-scale component in the near-bottom boundary layer. Thus, by analogy with the two-layer case (Part 1) the ‘displacement’ effect takes place here. As the height of the relief inhomogeneities increases the large-scale baroclinic motion in the bottom layer decreases, which, in turn, causes a decrease of the small-scale component. The resulting effect is that the strong relief displaces the baroclinic mode from the near-bottom layer.

A more accurate analysis of baroclinic modes over a strong relief carried out in §§ 5, 6, and 7 reveals the existence of a kind of resonance similar to that in the two-layer model (Part 1). Namely, for $\gamma = O(\alpha^{-1/2}) \ll 1$ there exist isolated values of the phase velocity $c_x = \sigma/k = c_r$ for which the amplitude of the near-bottom small-scale component increases strongly compared to the non-resonance case $c_x \neq c_r$, and the small-scale velocity exceeds the large-scale one in the near-bottom boundary layer. Moreover, in contrast with the non-resonance case, the large-scale component has a local maximum at the bottom. As a result, the mode intensifies strongly near the bottom. The ‘transition’ from the resonance regime to the non-resonance case takes place in a small interval of the values of c_x of length $\alpha^{-1} \ll 1$ near the resonance value c_r . Thus, one can assume that the resonance effect is dynamically unimportant because only a countable set of the values of c_x leads to resonance (see (6.1)) and a continuum of c_x is non-resonant.

At the same time, the classification of the relief for $N = \text{const}$ differs significantly from that in the two-layer case. In the two-layer model the topography effect for $L \simeq L_i$ is determined by the parameter $\Delta = \delta/\alpha\beta$. In the case under consideration this effect depends on the parameter $\gamma = O(1/(\Delta\alpha^{1/2})) \ll \Delta^{-1}$, i.e. the ‘efficiency’ of the relief is substantially higher as compared to the two-layer case. For example, $\Delta \simeq 1$ corresponds to a moderate relief in the two-layer case and, at the same time, to a strong relief for $N = \text{const}$ because $\gamma \ll 1$ with $\Delta = 1$.

Another important distinction is the strong dependence of topographic mode frequency $\sigma_{tp}^{(0)}$ on the stratification. It readily follows from (3.18) and (4.4) that

$$\sigma_{tp}^{(0)} = O(\delta\alpha^{1/2}) \gg \delta \quad (8.3)$$

for $L \simeq L_i$. Recall that the topographic mode frequency in a two-layer ocean is of the order of δ irrespective of the density difference between the layers. One can say that the continuous stratification increases the topographic mode frequency as compared to the two-layer case.

Note that for the actual $N(z)$ profile this enhanced efficiency of the bottom relief can reduce considerably because the buoyancy frequency in the abyssal region is small. Accordingly, the parameter s in (3.10) determining the topography effect can also be very small.

Thus, we have considered the Rossby modes in two-layer and $N = \text{const}$ models. The natural question arises of what is the mode behaviour for the real continuous oceanic stratification which is localized mainly in the upper layer of the ocean separated by the main pycnocline from the deep abyssal region with very weak density gradients. The analysis of the small-scale component \tilde{p} for $\alpha \gg 1$ performed in §3 can be readily generalized to the case of variable N if $n(-1) = O(1)$. The approximate solution for \tilde{p} has the form (3.23) with the parameter α replaced by $\alpha n(-1) = HN(-H)/f_0 L_b$. The result is valid only if $\alpha n(-1) \gg 1$, i.e. the near-bottom layer thickness is much less than H . For the real ocean we have $H = 4$ km, $L_b = 10$ km, $f_0 = 10^{-4} \text{ s}^{-1}$, $N(-H) = 10^{-3} - 10^{-4} \text{ s}^{-1}$, i.e. the typical value of parameter $\alpha n(-1) = O(1)$ and therefore the small-scale component is *not* confined to a thin near-bottom boundary layer. At the same time, by analogy with the two-layer model the main pycnocline region characterized by strong density gradients would be expected to prevent the ingress of the small-scale motion into the upper layer. It is believed, therefore, that the mode structure in the real ocean is similar to that in two-layer model.

This work was supported by grants from Russian Foundation of Basic Research (94-05-17538a, 96-05-65209). The authors wish to thank Professor V. M. Volosov for very helpful comments on the manuscript and M. V. Dmitrieva for the help in preparation of this manuscript.

Appendix

Equations (6.8b) and (7.4c) can be reduced easily to the form

$$s_{n+1} + s_{n-1} - \frac{2n}{B_0} s_n = J_n(B_0), \quad (\text{A } 1)$$

$$\bar{s}_{n+1} + \bar{s}_{n-1} - \frac{2n}{B_0} \bar{s}_n = n J_n(B_0). \quad (\text{A } 2)$$

The solution to (A1) is sought in the form

$$s_n = p_n J_n(B_0) + q_n Y_n(B_0), \quad (\text{A } 3)$$

where $J_n(B_0)$ and $Y_n(B_0)$ are linearly independent solutions of (A 1) with zero right-hand side; and p_n and q_n must to be determined.

Substitution of (A 3) into (A 1) yields

$$p_{n+1} J_{n+1}(B_0) + q_{n+1} Y_{n+1}(B_0) + p_{n-1} J_{n-1}(B_0) + q_{n-1} Y_{n-1}(B_0) - \frac{2n}{B_0} (p_n J_n(B_0) + q_n Y_n(B_0)) = J_n(B_0). \quad (\text{A } 4)$$

Using the identities

$$\frac{2n}{B_0} p_n J_n(B_0) = p_n J_{n+1}(B_0) + p_n J_{n-1}(B_0), \quad (\text{A } 5a)$$

$$\frac{2n}{B_0} q_n Y_n(B_0) = q_n Y_{n+1}(B_0) + q_n Y_{n-1}(B_0) \quad (\text{A } 5b)$$

we rewrite (A 4) as

$$\gamma_n J_{n+1}(B_0) - \gamma_{n-1} J_{n-1}(B_0) + \delta_n Y_{n+1}(B_0) - \delta_{n-1} Y_{n-1}(B_0) = J_n(B_0), \quad (\text{A } 6)$$

where

$$\gamma_n = p_{n+1} - p_n, \quad \delta_n = q_{n+1} - q_n. \quad (\text{A } 7a, b)$$

We assume γ_n and δ_n to satisfy the equations

$$\gamma_n J_n(B_0) + \delta_n Y_n(B_0) = 0, \quad (\text{A } 8a)$$

$$\gamma_n J_{n+1}(B_0) + \delta_n Y_{n+1}(B_0) = J_n(B_0) \quad (\text{A } 8b)$$

ensuring the validity of (A 6) for any n . It follows from (A 8) that

$$\gamma_n = \frac{\pi B_0}{2} J_n(B_0) Y_n(B_0), \quad (\text{A } 9a)$$

$$\delta_n = -\frac{\pi B_0}{2} J_n^2(B_0). \quad (\text{A } 9b)$$

The functions γ_n and δ_n can be readily found from (A.7) and (A.9):

$$p_n = p_1 + \frac{\pi B_0}{2} \sum_{k=1}^{n-1} J_k(B_0) Y_k(B_0), \quad (\text{A } 10a)$$

$$q_n = q_1 - \frac{\pi B_0}{2} \sum_{k=1}^{n-1} J_k^2(B_0), \quad (\text{A } 10b)$$

where p_1 and q_1 are arbitrary constants. Taking into consideration (6.8a) and the boundedness of s_n as $n \rightarrow \infty$ we obtain

$$p_1 = q_1 Y_0(B_0)/J_2(B_0), \quad q_1 = \frac{\pi B_0}{2} \sum_{k=1}^{\infty} J_k^2(B_0). \quad (\text{A } 11a, b)$$

Substitution of (A 10) and (A 11) into (A 3) results in

$$s_n = \frac{\pi B_0}{2} \left\{ J_n(B_0) \left[\frac{2}{\pi B_0} p_1 + \sum_{k=1}^{n-1} J_k(B_0) Y_k(B_0) \right] + Y_n(B_0) \sum_{k=n}^{\infty} J_k^2(B_0) \right\} \quad (\text{A } 12)$$

A similar solution to (A 2) can be obtained like manner.

REFERENCES

- GRADSHTEYN, S. & RYZHIK, I. W. 1965 *Tables of Integrals, Series and Products*, 4th Edn. Academic.
 DICKSON, R. R. 1983 Global summaries and intercomparisons: flow statistics from long-term current meter moorings. In *Eddies in Marine Science* (ed. A. Robinson). Springer.
 MCWILLIAMS, J. C. 1974 Forced transient flow and small-scale topography. *Geophys Astrophys. Fluid Dyn.* **6**, 49.
 PEDLOSKY, J. 1979 *Geophysical Fluid Dynamics*. Springer.

- REZNIK, G. M. 1986 Rossby waves and synoptic variability of the ocean. Doctoral Dissertation, Moscow, IO RAS (in Russian).
- REZNIK, G. M. & TSYBANEVA, T. B. 1999 Planetary waves in a stratified ocean of variable depth. Part 1. Two-layer model. *J. Fluid Mech.* **388**, 115.
- RHINES, P. B. & BRETHERTON, F. 1973 Topographic Rossby waves in a rough-bottomed ocean. *J. Fluid Mech.* **61**, 583.
- SAMELSON, R. M. 1992 Surface-intensified Rossby waves over rough topography. *J. Mar. Res.* **50**, 367.
- SENGUPTA, D., PITERBARG, L. I. & REZNIK, G. M. 1992 Localization of topographic Rossby waves over random relief. *Dyn. Atmos. Ocean.* **17**, 1.
- SUAREZ, A. 1971 The propagation and geometry of topographic oscillations in the ocean. PhD thesis, Department of Meteorology, MIT.
- VOLOSOV, V. M. 1976a Nonlinear topographic Rossby waves. *Oceanology* **16** (3), 389 (in Russian).
- VOLOSOV, V. M. 1976b On the nonlinear theory of topographic Rossby waves. *Oceanology* **16** (5), 741 (in Russian).
- VOLOSOV, V. M. & ZHDANOV, M. A. 1980a Linear theory of large-scale flows over an anisotropic bottom relief in a two-layer model of the ocean. *Oceanology* **20** (1), 5 (in Russian).
- VOLOSOV, V. M. & ZHDANOV, M. A. 1980b Linear theory of large-scale flows over an anisotropic bottom relief in a continuously stratified model of the ocean. *Oceanology* **20** (4), 581 (in Russian).
- VOLOSOV, V. M. & ZHDANOV, M. A. 1982 Nonlinear theory of large-scale flows over an anisotropic bottom relief in a two-layer model of the ocean. *Oceanology* **22** (5), 698 (in Russian).
- VOLOSOV, V. M. & ZHDANOV, M. A. 1983 Nonlinear theory of large-scale flows in a continuously stratified model of the ocean. *Oceanology* **23** (2), 204 (in Russian).
- WUNSCH, C. 1981 Low-frequency variability of the sea. In *Evolution of Physical Oceanography. Scientific Surveys in Honor of Henry Stommel*, p. 342. MIT.
- WUNSCH, C. 1983 Western Atlantic Interior. In *Eddies in Marine Science*, p. 46. Springer.
- ZHDANOV, M. A. 1987 On synoptic-scale motions in a two-layer ocean with uneven bottom. *Oceanology* **27** (3), 363 (in Russian).